Bachelor Thesis

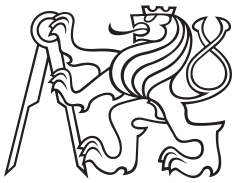

Czech Technical University in Prague

F3

Faculty of Electrical Engineering

Dynamic Range of Photomultipliers in Pulse Mode

Daniel Veškrna

Supervisor: Ing. Jakub Cikhardt, Ph.D.

May 2021

Acknowledgements

I would like to thank very much my supervisor Ing. Jakub Cikhardt, Ph.D. for his guidance and willingness throughout making this thesis. I would also like to thank the members of the hot plasma physics experimental group at the Department of Physics at the Faculty of Electrical Engineering CTU in Prague for helping me perform the experiments.

Declaration

I declare that the presented work was developed independently and that I have listed all sources of information used within it in accordance with the methodical instructions for observing the ethical principles in the preparation of university theses.

In Prague on May 21, 2021

Abstract

This thesis is devoted to the experimental evaluation of the dynamic range of photomultiplier tubes used for neutron detection. It aims to assess their sensitivity, linearity, relative gain, and transition time and the difference between individual photomultipliers. The knowledge of how the photomultiplier tubes behave under specific circumstances is essential to correctly use them during the experiment. For this purpose, two independent experiments were performed.

The first one used a plasma focus to produce hard x-ray and neutron pulses. At several supply voltages, the individual photomultiplier tubes showed clear differences between responses to the incoming signal. Their sensitivity, saturation levels, and linearity were described, although a larger number of tests would yield more conclusive results. The second experiment used a neodymium laser to measure the relative gain and transition time. The relative gain results correlated with the findings from the first experiment. The probable cause behind the differences between individual photomultipliers was found to be the degradation of the photocathode. The transition time among the photomultiplier tubes was practically the same. These findings together with the algorithms used to process the data can serve to make the upcoming experiment results more accurate.

Keywords: photomultiplier tube, scintillator, neutron, plasma focus

Supervisor: Ing. Jakub Cikhardt, Ph.D.

Abstrakt

Tato práce je věnována experimentálnímu vyhodnocení dynamického rozsahu fotonásobičů používaných k detekci neutronů. Jejím cílem je vyhodnotit jejich citlivost, linearitu, relativní zesílení a tranzitní čas a rozdíl mezi jednotlivými fotonásobiči. Znalost toho, jak se fotonásobiče chovají za konkrétních okolností, je nezbytná pro jejich správné použití během experimentu. Za tímto účelem byly provedeny dva nezávislé experimenty.

První z nich pomocí plazmatického fokusu produkoval tvrdé rentgenové a neutronové impulsy. Za různých napájecích napětích se ukázalo, že fotonásobiče vykazovaly jasné rozdíly mezi odezvami na příchozí signál. Byla popsána jejich citlivost, úrovně saturace a linearita, ačkoli větší počet testů by přinesl přesvědčivější výsledky. Druhý experiment používal neodymový laser ke změření relativního zesílení a tranzitního času. Výsledky relativního zesílení korelovaly se závěry z prvního experimentu. Pravděpodobnou příčinou rozdílů v parametrech mezi jednotlivými fotonásobiči byla degradace fotokatody. Tranzitní čas se mezi fotonásobiči prakticky nelišil. Tato zjištění spolu s algoritmy používanými ke zpracování dat mohou posloužit k většímu zpřesnění výsledků v nadcházejících experimentech.

Klíčová slova: fotonásobič, scintilátor, neutron, plazmatický fokus

Překlad názvu: Dynamický rozsah fotonásobičů v impulsním režimu

Contents

1 Introduction **1**

1.0.1 Aim of thesis 1

1.0.2 Layout of thesis 2

1.0.3 Personal contributions 2

2 Motivation **3**

2.1 Neutron sources 3

2.1.1 Spontaneous fission 4

2.1.2 Radioisotope (α, n) sources . . 4

2.1.3 Photoneutron sources 4

2.1.4 Reactions from accelerated charged particles 5

3 Methods of neutron detection **9**

3.1 Introduction 9

3.2 Slow neutron detection methods 10

3.2.1 Gas slow neutron detectors . . 11

3.2.2 Solid slow neutron detectors . 12

3.2.3 Liquid slow neutron detectors 12

3.3 Fast neutron detection methods 13

3.3.1 Detectors based on neutron moderation 13

3.3.2 Fast neutron-induced reaction detectors 14

3.4 Fast neutron scattering detectors 15

3.4.1 Bubble detectors 17

4 Scintillation detector principle **19**

4.1 Introduction 19

4.2 Scintillators and scintillation process 19

4.2.1 Organic scintillators 21

4.2.2 Inorganic scintillators 22

4.3 Photomultiplier tube 22

4.3.1 The photocathode 23

4.3.2 The electron multiplier 24

5 Experimental testing of PM tubes **27**

5.1 PFZ-200 experiment 27

5.1.1 Experiment setup 29

5.1.2 Results 30

5.2 Neodymium laser experiment . . . 33

5.2.1 Experiment setup 34

5.2.2 Results 35

5.3 Discussion 38

6 Conclusion **41**

Bibliography **43**

Project Specification **45**

Figures

2.1 Plasma focus device at Department of Physics laboratory of Faculty of electrical Engineering, CTU in Prague (photo credit: Bc. Petr Neugebauer). 6

2.2 Plasma focus scheme (inspiration from [1]); 1 - anode, 2 - insulator, 3 - cathode, 4 - vacuum chamber, Is - spark gap, C - capacitor bank, a - discharge phase, b - acceleration phase, c - radial movement of the layer and creation of the plasma focus. 7

3.1 Cross section of typical elements used in neutron gas detectors. Dashed and dotted lines corresponds to fission and nuclear recoil reactions. These are the characteristic reactions for slow and fast neutrons respectively. Source: [2] 10

3.2 Polyethylene moderator counter of Ag in Department of Physics laboratory of Faculty of electrical Engineering, CTU in Prague 14

3.3 Typical cylindrical plastic scintillator (Source: NuviaTECH instruments NuDET plastic specification sheet) 16

4.1 Cross section of the scintillation detector 20

4.2 Schematic of a photomultiplier tube coupled to a scintillator. By Qwerty123uiop, CC BY-SA 3.0, https://commons.wikimedia.org/w/index.php?curid=62426194 23

4.3 Typical types of PM tubes with different shape, structure, effective area, etc. Hamamatsu Photonics Deutschland GmbH, https://www.hamamatsu.com 23

4.4 Typical PM voltage divider circuit using negative high voltage. By Qwerty123uiop - Own work, CC BY-SA 4.0, https://commons.wikimedia.org/w/index.php?curid=38349029 25

5.1 Exemplary signal from scintillation detector on the PFZ-200. The first peak around 0 ns are the HXR and the second dual peak are the neutrons from two consequent pinches. 28

5.2 Exemplary signal from scintillation detector on the PFZ-200 where the PM tube got saturated. 28

5.3 Scintillation detector in its housing. 29

5.4 Setup of four scintillation detectors in a Faraday cage, numbered PM1-PM4 from the left. 29

5.5 HXR signal amplitude comparison of four used PM tubes at 1.4 kV supply voltage. The red arrows marks a signal where the PM tube was in saturation. 30

Tables

5.6 HXR signal amplitude comparison of four used PM tubes at 1.2 kV supply voltage. The red arrows marks a signal where the PM tube was in saturation. 31

5.7 Dependence of the neutron signal from the PM tubes on the total neutron yield at 1.4 kV PM tube supply voltage. 33

5.8 Dependence of the neutron signal from the PM tubes on the total neutron yield at 1.2 kV PM tube supply voltage. 33

5.9 Block scheme of the experiment setup with cable measurements. . . 34

5.10 Response of the photodiode to the laser pulse. 35

5.11 Response of the PM tube to the laser pulse. 35

5.12 Effect of supply voltage on the relative gain of the PM tubes. 36

5.13 Comparison of the gain results in logarithmic scale. 37

5.14 Effect of supply voltage on the transition time of the PM tubes. . . 38

Chapter 1

Introduction

This thesis is devoted to the experimental evaluation of the dynamic range of photomultiplier (PM) tubes used for neutron detection. PM tube is a device that converts incident photons into electrons and multiplies them into a measurable electrical signal [3]. To detect neutrons, it is usually coupled to a scintillator, forming a scintillation detector. It converts them into visible photons that enter the PM tube. To do that, it uses a process of scintillation, which is a flash of light produced in a transparent material by the passage of a particle [4], in this case a neutron or a hard X-ray photon (HXR).

1.0.1 Aim of thesis

The aim of this thesis is to use several PM tubes that are used as diagnostics to detect neutrons in the Plasma Focus Laboratory at the Department of Physics FEE CTU and to evaluate their dynamic range. Since the process of the formation of a plasma focus is quite unpredictable in nature, correctly setting and synchronizing the PM tube is essential. To do so, a knowledge of how the PM tube behaves at different conditions is needed. This is achieved by conducting two experiments using the PFZ-200 device and a neodymium laser. The sensitivity and linearity of the PM tube at different supply voltages are addressed, as well as the saturation gain and transition time.

1.0.2 Layout of thesis

This thesis is divided into 6 chapters. The topic of neutron sources as a motivation and overview of the methods of neutron detection are described in chapters 2 and 3. Chapter 4 provides a more in-depth look into how the scintillation detector works. All experiments and their results are in chapter 5 and chapter 6 is the conclusion of this thesis.

1.0.3 Personal contributions

The author of this thesis actively participated in the experiments on the PFZ-200 plasma focus. He helped to operate the device and record the data. He operated the neodymium laser and relevant equipment to test the PM tubes. He wrote the algorithms to subsequently process the data, which he evaluated to obtain the results presented in this work.

Chapter 2

Motivation

Neutrons as a field of study in general are nowadays topics of high interest. They play a crucial role in research from nuclear and elementary particle physics, chemistry, and materials science to engineering and life sciences. For example, subcritical experiments, r-process, neutronics, and so on, just to mention few. Especially in the search for 'green' energy sources, neutrons pose a major problem in thermonuclear reactors, as they can induce serious degradation of constructional materials [5]. Therefore, neutron diagnostics and study of neutron-proof materials are important.

The key topic of this thesis is the evaluation of the dynamic range of PM tubes used for neutron detection in the plasma focus laboratory at the Department of Physics, FEE CTU. Therefore, a brief discussion on the topic of neutron sources is only appropriate. The main source for this chapter and the upcoming ones is a book by Knoll that heavily covers the major neutron topics [3]. Other sources are [6, 7].

2.1 Neutron sources

Nuclei with enough excitation energy can decay by neutron emission, but there is no convenient radioactive decay process to create such energetic nuclei. Consequently, practical isotope sources of neutrons are not available in the same sense as gamma-ray sources are, which limits the choice to either spontaneous fission or nuclear reaction-based processes.

2.1.1 Spontaneous fission

A useful isotopic neutron source are the transuranic heavy nuclides. In each fission event, they emit several fast neutrons as well as gamma rays and beta activity products. Such isotopes can be encapsulated in a sufficiently thick container that only fast neutrons and gamma rays can escape.

The most common spontaneous fission source is ^{252}Cf. It is one of the most produced transuranic isotope with a reasonable half-life of 2.65 years. The neutron yield is 0.116 n/s per Bq or $2.30 \cdot 10^6$ n/s per microgram of the sample. Neutrons come from the dominant alpha decay and spontaneous fission and peak between 0.5 and 1 MeV, but a significant amount is as high as 8 or 10 MeV. ^{252}Cf sources involve small amounts of active material (in micrograms) which makes it a very convenient neutron source.

2.1.2 Radioisotope (α, n) sources

An (α, n) reaction can be used as a neutron source, because energetic alpha particles are available from the direct decay of a number of convenient radionuclides. When a suitable target material is used, such as beryllium, neutrons are produced through the reaction

$$ {}^{4}_{2}\alpha + {}^{9}_{4}\mathrm{Be} \longrightarrow {}^{12}_{6}\mathrm{C} + {}^{1}_{0}n \tag{2.1} $$

which has a Q-value of +5.71 MeV. The alpha emitters, mostly actinide elements, are usually mixed with beryllium in the form of alloy. Other reactions are occasionally used, but beryllium has the highest neutron yield per unit alpha activity in comparison.

2.1.3 Photoneutron sources

It is possible to supply sufficient excitation energy to a target nucleus via a gamma-ray absorption for it to emit a neutron. Practically, only ^{9}Be and ^{2}H are of any significance. The reaction is energetically possible only if the gamma-ray photon has the energy of at least the negative Q-value of

the reaction itself. Therefore, only relatively high-energy gamma rays can be applied. The advantage is that if the gamma rays are monoenergetic, the neutrons are also monoenergetic. The disadvantage is that very large gamma-ray activity is needed for any reasonable neutron source intensity. Because of that, neutrons appear in an intense gamma-ray background which complicates further measurements.

2.1.4 Reactions from accelerated charged particles

Reactions involving incident protons, deuterons, and so on must rely on artificial acceleration, because they need to overcome the electrostatic forces. When they do, a fusion can occur. There are two basic types of fusion reactions: first preserves the number of protons and neutrons and second involves a conversion between protons and neutrons. The second type reactions are crucial to the initiation of star burning [8]. The reactions of the first type are most important for practical fusion energy production. The two most commonly used are the D - D reaction and the D - T reaction (D stands for deuterium and T for tritium):

$$\begin{aligned} \text{D - D:} \quad & {}^{2}_{1}\mathrm{H} + {}^{2}_{1}\mathrm{H} \longrightarrow {}^{3}_{2}\mathrm{He} + {}^{1}_{0}n \\ \text{D - T:} \quad & {}^{2}_{1}\mathrm{H} + {}^{3}_{1}\mathrm{H} \longrightarrow {}^{4}_{2}\mathrm{He} + {}^{1}_{0}n \end{aligned} \tag{2.2}$$

To create a significant neutron yield, the deuterons need not be accelerated to a very high energy. Compact neutron generators can consist of a sealed tube with the ion source and target, together with a high-voltage generator creating a potential of about 100-300 kV for the acceleration. The produced neutrons have about the same energy as the Q-value of the reaction (near 3 MeV for the D - D reaction and 14 MeV for the D - T reaction). Other examples of charged-particle-induced reactions are ^{9}Be(d, n), ^{7}Li(p, n), and ^{3}H(p, n), but a higher incident particle energy is needed. Only large accelerator facilities such as cyclotrons or Van de Graaf accelerators are capable of such energy requirements.

Plasma focus

In this work, the PM tubes were tested on a plasma focus (PF) device PFZ-200 at FEE CTU in Prague. It is a relatively small device (see Fig. 2.1) capable of producing a plasma column with 200 - 250 kA of current. The PF is a type of Z-pinch where plasma is produced by an electric discharge in gas. It was derived from the first experiments (where the current flowed along the z axis) by modifying the placement of the insulator [1].

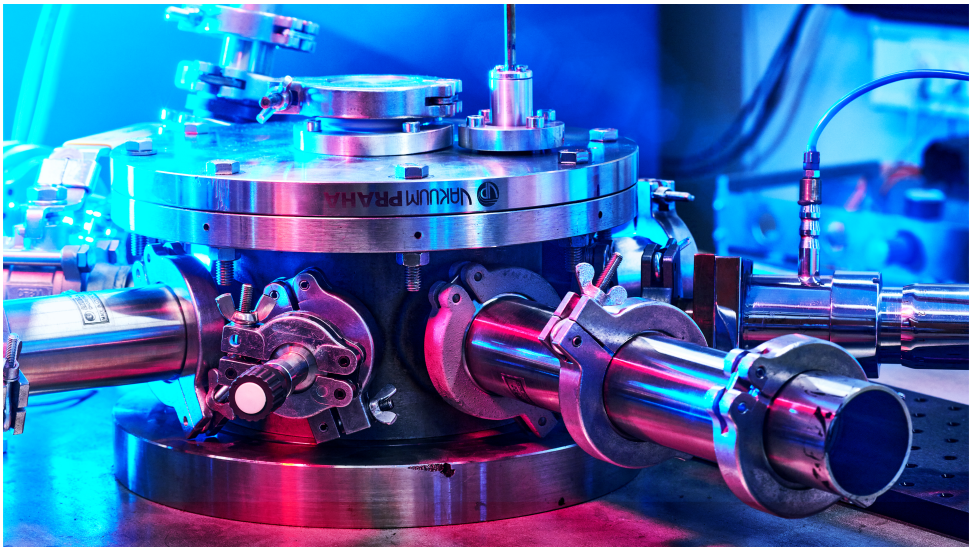

Figure 2.1: Plasma focus device at Department of Physics laboratory of Faculty of electrical Engineering, CTU in Prague (photo credit: Bc. Petr Neugebauer).

A typical PF consists of the following basic elements (see Fig. 2.2):

- Electrical energy storage - capacitor bank (C).
- Electrical circuit - low-inductive spark gap (Is), cables between the bank and the current collector.
- An anode (1) separated from a cathode (3) by a cylindrical insulator (2) in the vacuum chamber (4).

The vacuum chamber is first pumped out to high vacuum (about 10^{-3} Pa) and then filled with different types of gases as required. To have a fusion reaction, deuterium is used, sometimes together with small amount of an

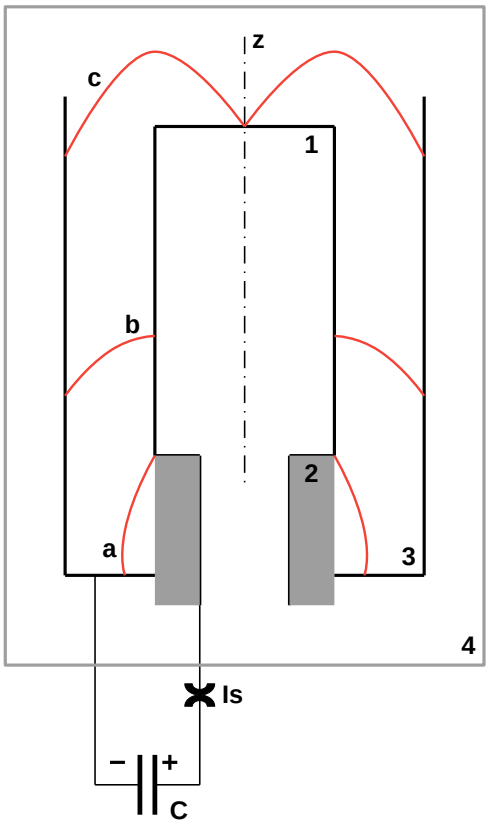

Figure 2.2: Plasma focus scheme (inspiration from [1]); 1 - anode, 2 - insulator, 3 - cathode, 4 - vacuum chamber, Is - spark gap, C - capacitor bank, a - discharge phase, b - acceleration phase, c - radial movement of the layer and creation of the plasma focus.

inert gas, such as argon for diagnostic purposes. In our experiments with PFZ-200, deuterium with a pressure of 340 Pa was used.

The creation of the plasma focus discharge goes as follows (Fig. 2.2): Energy from the capacitor bank is discharged by triggering the spark gap. As the voltage grows on the electrodes, electrical discharge forms in the gas along the insulator. The plasma layer is formed and the electrical discharge current increases (phase a). This forms a current sheath that detaches from the insulator, ionizes, and sweeps through the gas while accelerating along the electrodes (phase b). With correct power source and electrode setting, as the current builds up and the sheath reaches the end of the anode, the current is at its maximum. The axial component of the current sheath density starts forming the azimuthal component of the magnetic field which causes movement of the current sheath towards the axis of the electrodes (phase c). This results in compression and heating of the plasma, forming the plasma focus with high particle density on the axis of the anode. Particles of concentration of 10^{19} per cm^3 are heated to temperatures typically up

to 1 keV (over 11 mil. Kelvin) and the current density reaches a value of more than 10^7 A/cm^2. In the PFZ-200, the temperature typically reaches few hundreds eV.

Created current instabilities, rapid plasma resistivity increase, and current decrease is followed by fast dissipation of the magnetic energy of the current into plasma. This enables the emergence of accelerated charged particles, electrons and ions, HXR pulses, as well as neutron radiation pulses (in the case of deuterium gas). The final stage of this phenomenon takes from several to hundreds of nanoseconds (few ns maximum in PFZ-200).

Many other types of devices capable of thermonuclear fusion exist. Some of them have the potential to create controlled nuclear fusion (i. e., tokamak), but a lot of work is still required to reach this vision of energy independence. However, experiments with smaller and simpler apparatuses such as the PFZ-200, Z-pinches, or laser plasma systems can lead to further understanding of the principles necessary to reach that goal.

Chapter 3

Methods of neutron detection

3.1 Introduction

Since neutrons carry no charge, they can travel through many centimeters of matter without significant interaction. Therefore, common radiation detectors cannot be used. Neutron detectors usually rely on a target material that neutrons can interact with. When they do, the result is either one or more secondary radiations with the neutron disappearing completely, or a significant change in neutron energy or direction.

The secondary radiation usually consists of energetic charged particles, such as protons or alpha particles. They are created either via neutron-induced nuclear reactions or by neutron collisions, where the recoil particles are the nuclei of the absorbing material itself. These particles can be detected by conventional radiation detectors.

Types of neutron interactions vary with neutron energy levels. Therefore, we usually divide them into *slow neutrons* and *fast neutrons*. The point of division is about 1 MeV (electron volts), which is the energy of the abrupt drop in the absorption cross section of cadmium. This is so called the *cadmium cutoff* energy. Physical interpretation of the cross section would be the probability per unit path length that any type of interaction will occur. Figure 3.1 shows cross sections for typical elements used as neutron converters. Each interaction then has its own cross section with its units of area, traditionally being measured in units of *barn* ($10^{-28}\mathrm{m}^2$).

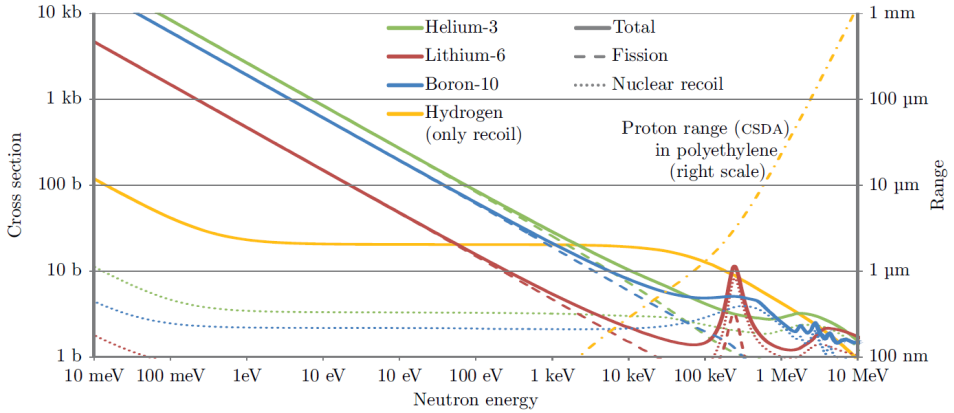

Figure 3.1: Cross section of typical elements used in neutron gas detectors. Dashed and dotted lines corresponds to fission and nuclear recoil reactions. These are the characteristic reactions for slow and fast neutrons respectively. Source: [2]

Many detection methods have been developed for each energy region so far. The most relevant for this work and the most common of them will be discussed in this chapter. As stated before, main inspiration for this chapter comes from the book by Knoll [3], if not stated otherwise.

3.2 Slow neutron detection methods

Slow neutrons have small kinetic energy which presents a problem for their detecting. Most of the interactions happen via elastic scattering of the absorber nuclei and very little energy is being transferred to the nucleus. This tends to bring the neutron to thermal equilibrium before other types of reactions can occur. Therefore, those interactions cannot be used to detect them.

The main role here plays neutron-induced reactions that produce secondary radiation with enough energy to be detected. Because of the small neutron energy, for them to be energetically possible, a positive Q-value is required. That means the reaction must be exothermic. Furthermore, most of the secondary radiation is in the form of gamma rays (radiative capture reaction (n, γ)), which makes measuring neutron energy very problematic, because this reaction occurs in the resonance area. Reactions resulting in charged particles such as (n, α), (n,p), or (n, fission) are hence much more appealing.

To measure the kinetic energy of slow neutrons, rather complex systems are required, therefore will be postponed. Methods that only indicate the detection of neutrons can be divided into *passive* and *active*. Passive detectors include, for example, activation foils, but they will be skipped as well. We will also discuss common types of active detectors that produce a current or pulse signal by each neutron. Fast neutrons are of more importance for this work and will be subject of the next part.

3.2.1 Gas slow neutron detectors

Using gas as a detection medium has important consequences in detector design. If a neutron reaction occurs, its product particles need to be stopped to capture their full kinetic energy. The detector must have a large enough active volume to do that, because the secondary radiation can travel significant distances (typically several centimeters) in comparison to the size of the detector itself. This is not an issue in solid detectors, because the range of any of the reaction products does not exceed a few tenths of a millimeter. If those conditions are satisfied, the response function of the detector is a single full-energy peak. However, if the particles do not deposit all energy, the peak is not as clearly distinguishable from other low-amplitude events (such as gamma-ray-induced processes). That is indeed undesirable.

There are several types of reactions according to which the gas is selected and used in the gas chambers. The most popular is probably the ^{10}B(n,α) reaction. Its Q-value is very large (up to 2.792 MeV) compared to the incoming energy of the slow neutron. The cross section for slow neutrons is fairly large as well at 3840 barns and drops rapidly with increasing neutron energy. A widely used boron detector is the BF_3 proportional tube, where boron tri-fluoride is both the target for slow neutron conversion to secondary particles and the proportional gas to capture their energy. It has poor performance at high pressures, so the typical tube pressure is at 0.5-1.0 atm. Because of its high boron concentration and other superior properties, BF_3 is generally the best gas to use.

Another widespread gas as a detection medium is helium through the ^{3}He(n,p) reaction. Compared to the boron reaction, the neutron cross section is significantly higher at 5330 barns, but the Q-value is lower at 0.764 MeV. When the maximum detection efficiency is important, ^{3}He performs better than BF_3, because it can operate at higher pressures. On the contrary, the small Q-value makes gamma-ray discrimination more difficult. Helium is also a noble gas and its relatively expansive, which plays a role in its application. Despite that, ^{3}He proportional tube detectors came into common use.

3.2.2 Solid slow neutron detectors

As stated before, the advantage of solid material as a target or conversion medium is the small active volume required. Any reactions happen much more frequently, therefore only a thin layer of the material is needed.

Popular detectors using solid forms of lithium are based on the ^{6}Li(n,α) reaction. It has a high Q-value of 4.78 MeV and the cross section is 940 barns. Even though the lower level of the cross section is a disadvantage, it is being compensated by the higher Q-value and the fact that lithium can be in solid state. Quite common detectors based on this reaction are, for example, scintillators using crystalline lithium iodine (more on scintillation in chapter 4). Its large density makes it very efficient for slow neutron detection and allows for crystals not to be very large. Large Q-value offers an advantage against gamma-ray and other low-amplitude reactions. Lithium iodide is, however, highly hygroscopic and must be hermetically sealed from water vapor exposure. This is not a problem for glass scintillators using lithium-containing glass fibers, which are also widely used for slow neutron detection.

Relatively large fission cross section of ^{233}U, ^{235}U, and ^{239}Pu makes them usable as the basis of slow neutron detectors. Q-value of the fission reaction is approximately 200 MeV, which is enormous compared to the reactions discussed thus far. The resulting output pulses of these detectors can often be orders of magnitude higher than other competing reactions, including the natural alpha radiation of these fissile nuclides. The most common fission detectors are ionization chambers with fissile deposit coated inner surfaces.

3.2.3 Liquid slow neutron detectors

Liquid forms of some elements suitable for slow neutron detection can be sometimes easily achievable and therefore desirable. Being much denser than gas, the liquid detection medium offers similar advantages as the solid one in comparison. Scintillators with ^{6}Li with 0.15% concentration are being used commercially. They can be also used with gadolinium solution at about 0.5% concentration. ^{157}Gd has a cross section for thermal neutron capture of 255 000 barns, which is the highest in almost any material found. Neutron absorption results in gamma-ray and conversion electron production. Because of the rather low electron energy of 72 keV, gamma-ray background reactions pose more of a problem compared to the heavy charged particles resulting reactions discussed previously.

3.3 Fast neutron detection methods

On the contrary to slow neutrons, elastic neutron scattering plays an important role here. Now, neutrons can transfer enough kinetic energy to the scattering nucleus that the resulting recoil nuclei can be detected. The original neutron kinetic energy can be calculated from the recoil nuclei kinetic energy. The lighter the nuclei, the more kinetic energy can be transferred. Hydrogen is therefore the obvious choice. It has well-known energy dependency and a large cross section.

Fast neutrons can be detected using the reactions mentioned for slow neutrons as well. When the neutron energies are at least 10-100 keV, the energy of the reaction products is no longer negligible compared to the reaction Q-value. That means that the neutron kinetic energy can be deduced from the reaction products, because the Q-value can be simply subtracted.

Even though the kinetic energy of fast neutrons can be calculated retrospectively (which is rather complicated in the case of slow neutrons), in some cases only the measurement of neutron presence is required. The use of counters is therefore preferred. They record pulses from charged particles and are useful only for small changes in the neutron spectrum between measurements.

Detectors based on the principles mentioned above, as well as other commonly used types for fast neutron detection, such as bubble detectors, will be briefly discussed.

3.3.1 Detectors based on neutron moderation

Fast neutrons can be slowed down using a material called a moderator. The knowledge of slow neutron detection can be now applied with slight modification. The moderator is usually a type of hydrogen-containing material, because it can absorb neutron energy efficiently. The thickness of the moderator is a key thing to consider. The thicker the moderator, the lower the most probable neutron energy as it reaches the detector, but also the greater the chance it will never make it. Thickness for commonly used moderators, such as paraffin or polyethylene, ranges from a few centimeters for keV neutrons to tens of a centimeter for MeV neutrons. Figure 3.2 shows Ag counter detector that uses polyethylene as the moderator. Detectors can thus be tailored for efficient detection to the corresponding applications. Commonly used

moderation detectors are, for example, spherical dosimeters or long counters.

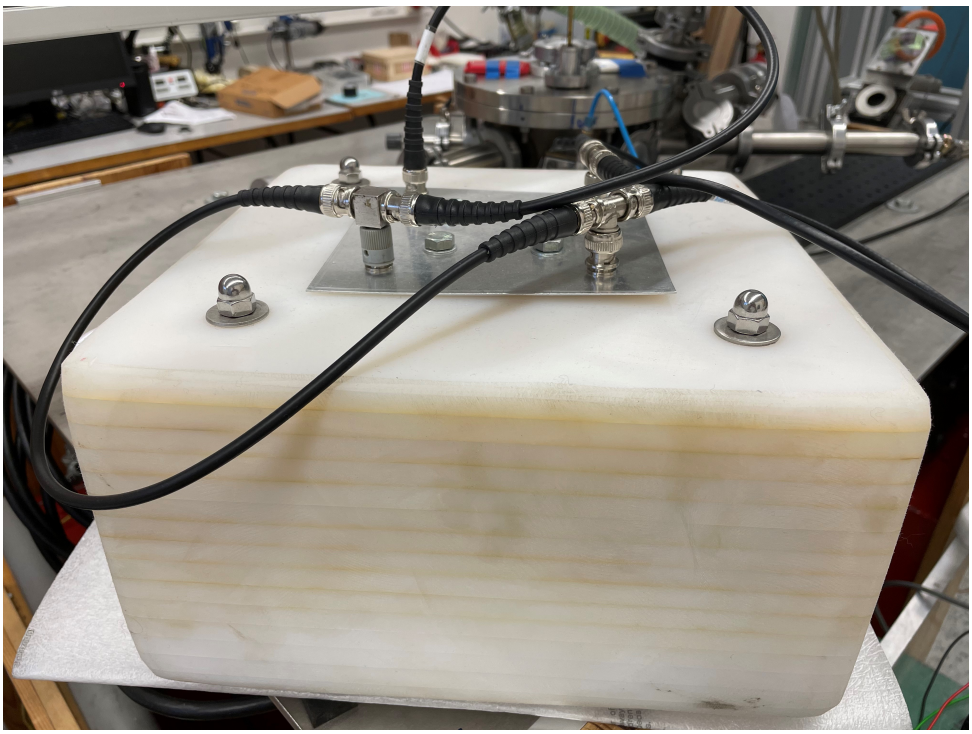

Figure 3.2: Polyethylene moderator counter of Ag in Department of Physics laboratory of Faculty of electrical Engineering, CTU in Prague

3.3.2 Fast neutron-induced reaction detectors

Since the incoming neutron energy is no longer negligible to the Q-value of the reaction, the kinetic energy of the neutron can be calculated. The same reactions as for slow neutrons apply and now by subtracting Q-value of the reaction from the energy of the reaction particle will give the incoming neutron energy. However, the cross sections for these reactions are orders of magnitude lower than for thermal (slow) neutrons, which means lower efficiency. Because of that, only ^{6}Li(n,α) and ^{3}He(n,p) reactions come into consideration, both discussed previously. Scintillators are often used for the lithium reaction, for example, iodide, glass or glass fiber scintillators. Other types, such as sandwich spectrometer, exists. The helium reaction is suitable for proportional counters, ionization chambers, semiconductor sandwich spectrometers, as well as scintillators.

As in the case of slow neutrons, fast neutrons can also induce radioactivity in certain materials. Activation counters utilize this and are commonly used. They are most suited for short pulses of fast neutrons.

Neutron detection by activation

The induced radioactivity can be measured and used to deduce information about the neutrons that caused it. Activation detectors are often used for slow neutron detection, because they have typically the highest cross section. However, reactions such as (n, p), (n, α), and (n, 2n) often require a threshold of minimum energy, therefore fast neutron detection is preferable.

The principles are again similar as for slow neutron detection. The activation material is usually a thin foil or a wire with small diameter. Related class of activation detectors are activation counters which are very useful for measuring bursts of fast neutrons typically produced in accelerators. The induced activity is then measured directly by a sensor placed in proximity to the activation material. More on fast neutron activation can be found here [9].

3.4 Fast neutron scattering detectors

As stated before, recoil particles from scattering interactions are detectable in this case, because fast neutrons have enough energy to transfer. Lighter nuclei can absorb more of this energy and they also behave similarly as protons or alpha particles. Most popular is hydrogen, but deuterium or helium are used as well. In the case of hydrogen scattering, the resulting recoil nucleus is called the recoil proton.

For all practical purposes, the target nuclei are at rest, therefore sum of the recoil nucleus and scattered neutron energy is equal to the incoming neutron kinetic energy, because Q-value of scattering is zero by definition. Recoil proton energy can range from zero to the full energy of the incoming neutron, so the average is about half of the original neutron. That means neutrons can be detected in the presence of low-energy background events or gamma rays, but it becomes harder below energies under a few hundred keV. By using pulse shape or rise time discrimination techniques, proton recoil detectors can detect neutrons with energies as low as 1 keV.

Proton recoil scintillators

Using scintillators is one of the easiest ways to use proton recoil in detection. Recoil protons are created in the scintillation material with an energy distribution from zero to full neutron energy. All recoil proton energy is then deposited in the scintillator, because the recoil proton travel distance is small compared to the detector dimensions (more on scintillation in chapter 4).

As can be expected, hydrogen-containing scintillators are among the most commonly used neutron scintillation detectors. There are many types of materials containing hydrogen used in scintillators that have been successfully used in a variety of applications. Organic crystals such as anthracene or stilbene have the largest light output of any organic scintillator, but are expensive and difficult to obtain in larger sizes. They are also prone to thermal and mechanical shock and their light output depends on the direction of the crystal axis. Plastic and liquid scintillators are much less expensive, come in many shapes and sizes, and their response is nondirectional. Therefore, they are more commonly used. Plastic scintillators use a matrix of polymerized hydrocarbon in which an organic scintillant is incorporated. An example of a plastic scintillator is in Fig. 5.3. Liquid scintillators combine organic scintillant dissolved in a hydrogen-containing solvent.

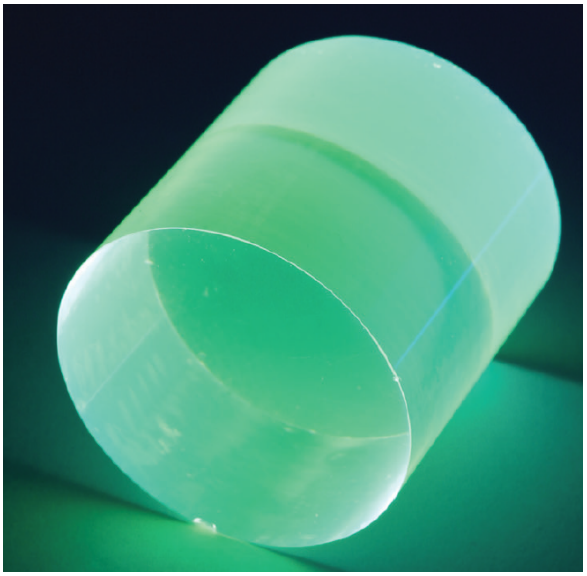

Figure 3.3: Typical cylindrical plastic scintillator (Source: NuviaTECH instruments NuDET plastic specification sheet)

Gas recoil proportional counters

Hydrogen, helium and methane or other hydrogen-containing gas can also be used to measure fast neutrons through the recoil process. Hydrogen has a simple response function, but organic gases often do not and their use is then much more complicated.

Since the gas has a low density, the scattered neutron has a much lower probability to undergo any other interaction, which makes the response function simpler. On the other hand, the efficiency of neutron detection in a first place is also very low, less than 1 % for hydrogen in MeV neutron energy range. Gas recoil proportional counters also have constructional criteria that, if not done well, can lead to detector failure. To the most important ones belong the purity of filler gas and leak-proof chambers.

3.4.1 Bubble detectors

Bubble detector uses a different mechanism to detect incoming neutrons - a fluid state transition. There are small droplets of fluid in a metastable ("superheated") state in the detector. To undergo a transition from liquid to vapor, the fluid needs a nucleation trigger. In this case, that trigger is so-called "thermal spike" - highly localized hot region created by a charged particle produced by neutron interaction (recoil ion). If this particle crosses the metastable droplet, the "thermal spikes" with a temperature above the superheat limit lead to the fluid transition [10]. The droplet flashes into a bubble of vapor up to a millimeter in diameter that can be then visually detected.

The liquid droplets, for example, of freon, are up to 100 μm in size. They are held in a polymer or gel matrix that is immiscible with the fluid. The matrix contains tens of thousands of droplets and is usually transparent. After vaporization, the bubbles can be held within the matrix or collected somewhere in the detector. More information about this interesting technology can be found in this paper [11]. Their usage as a personal neutron dosimeter and study of longevity of such device can be found here [12].

The charged particle must have enough energy to trigger bubble nucleation. Recoil nuclei created by fast neutron scattering can produce such energetic particles. The trigger sensitivity can become higher by increasing the liquid temperature, but also decreases as more droplets become bubbles while

measuring. Bubble detectors can also be made to detect lower energy neutrons by using fluid producing charged particles by neutron-induced reactions (for example, with chlorine). There are two basic types of bubble detection methods: passive and active.

Passive detection is the simplest, because the bubbles are counted manually or with a scanner. However, this poses a problem as the bubbles can overlap, resulting in increasing counting difficulty above hundreds bubbles in a typical few cubic meters of material. Because the fluid is held metastable at low pressure, the whole apparatus can be reset by increasing the pressure, causing the bubble to condense.

Active detection uses an acoustic sensor during the measurement. Fluid transitions produce a sound that can be picked up by the sensor and transformed into an electrical signal. Usually, a second acoustic sensor is placed somewhere else on the detector to compare both signals and distinguish only the bubble formation. Somewhat similar problem to the passive method can occur, when the sound of two bubbles overlap, causing distortion in counting.

Chapter 4

Scintillation detector principle

4.1 Introduction

A scintillation detector consists of two main parts: a scintillator and a photodetector (see fig. 4.1). The scintillator generates low energy photons in response to incident radiation. The photodetector, a photomultiplier tube in our case, then converts the photons to an electrical signal, which can be further processed. Both of those key components will be now further discussed. Main sources for this chapter are [3, 6, 13, 14].

4.2 Scintillators and scintillation process

Scintillation is a flash of light produced in a transparent material by the passage of a particle (an electron, an alpha particle, an ion, or a high-energy photon) [4]. It is the property of *luminescence* where the incident radiation generates light of a characteristic spectrum [15]. More specifically, it is the *fluorescence* and *phosphorescence* that play the major role here. They are both a type of *photoluminescence* which is a result of photon absorption and consequent emission of light. The emitted photons have typically longer wavelengths, thus lower energy than the absorbed photons.

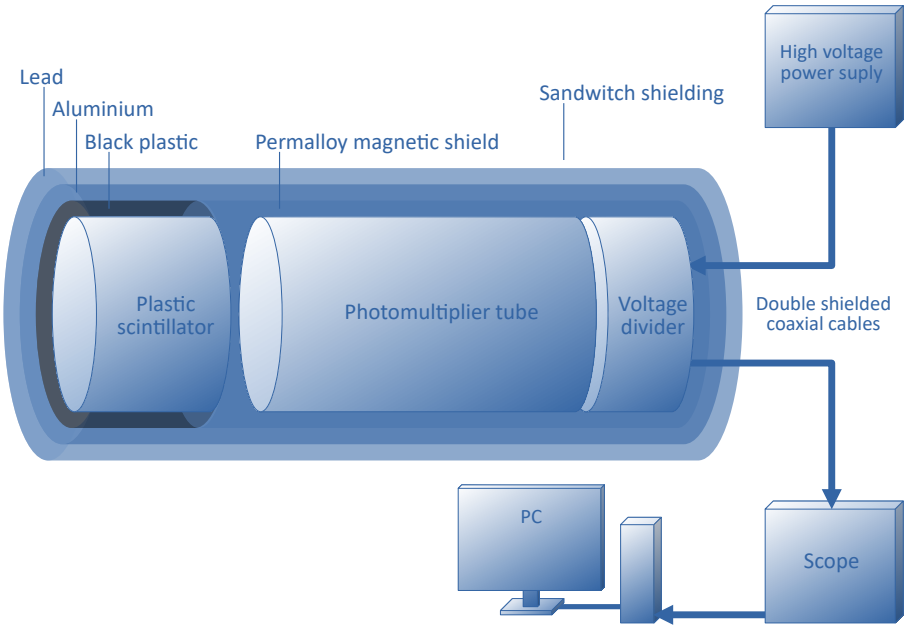

Figure 4.1: Cross section of the scintillation detector

Fluorescence is the prompt emission of visible radiation from a substance with a lifetime of nanoseconds. *Delayed fluorescence* has the same wavelength, but much longer emission time. Phosphorescence is the emission of longer wavelength light and has a much longer lifetime.

A scintillator is a material that exhibits scintillation. A good scintillator should convert as a large a fraction of the incident photons to prompt fluorescence, when used in pulse mode. The undesirable long-lived phosphorescence and delayed fluorescence will arrive randomly between pulses and will be often indistinguishable from a background noise. If present in a larger portion, the scintillator would suffer from the memory or "afterglow" effects of their longer lifetime emission. In scintillators operated in current mode, all emission components will contribute to the total light yield in proportion to their light intensity. However, in cases when the radiation intensity changes rapidly, they will suffer from the afterglow as well. Therefore, correct usage of the right type of scintillator is important.

Scintillators can be further divided into organic and inorganic. Both types and their examples will be briefly discussed in general. More information about the newest scintillation materials can be found here [16].

4.2.1 Organic scintillators

The process of fluorescence in organics occurs on a molecular level. Such an organic material can be therefore observed scintillating independently of its physical state - solid, liquid, or gaseous, like, for example, anthracene. This is in stark contrast to crystalline inorganic scintillators that require a regular crystalline lattice.

There are many types of organic scintillators. Pure organic crystals have really only two widespread examples - anthracene and stilbene. Although fragile and hard to make, they have the highest X-ray scintillation efficiency (or light output per unit energy) of any organic scintillator. Liquid scintillators are often the only practical solution in cases where large volume detectors are required, as they are quite inexpensive. Probably the most widespread are the plastic scintillators. They are easy to fabricate, come in different shapes and sizes, and are also relatively inexpensive. In cases where weakly penetrating particles, such as heavy ions, need to be detected, thin film scintillators with thickness as low as 20 μg/cm^2 play a unique role.

In terms of a time response of the organic scintillator, instantaneous forming of the luminescence states in a molecule and only prompt fluorescence can be assumed. Then the light pulse should be a very fast leading edge followed by a simple exponential decay. Prompt fluorescence intensity at time t is simply

$$I = I_0 e^{-t/\tau} \tag{4.1}$$

where τ is the fluorescence decay time, typically a few nanoseconds. However, there are cases when a more detailed model is required, counting in the finite time to populate the luminescent states and the slower emission of phosphorescence and delayed fluorescence.

The scintillation yield curve can be described by the sum of two exponential decays, corresponding to their photoluminescence types, called the fast and slow components. As the most observed light comes from the prompt fluorescence making the fast component, the slow component is often not of great consequence. However, the slow component light is unique to different kinds of particles. It can be therefore differentiated between particles, even if they deposit the same energy in the detector. This is called *pulse shape discrimination* and is important to distinguish gamma-ray events in neutron detection.

4.2.2 Inorganic scintillators

Inorganic scintillator needs a material not molecular in nature (like in organic scintillators), but with properties found in crystals to work [15]. The scintillation mechanism depends on the energy states determined by the crystal lattice. The material has to be either an insulator or a semiconductor and has to have added impurities (called *activators)* that enhance the probability of visible photon emission. Otherwise, in pure crystals, this process is quite inefficient. There are also a few types of gases that can be used. Overall, inorganic scintillators are not very neutron sensitive and thus not often used for neutron detection.

Inorganic scintillators can be divided into three main categories: inorganic crystals, gaseous, and glass scintillators. Inorganic crystals are grown in high temperature furnaces. The most common ones are from alkali halide metals, for example, NaI(Tl). One of their first application for X-ray detection is described here [17]. They are typically slower than organic ones, but have a high light yield. They are often hygroscopic and need to be housed in airtight containers. Gaseous scintillators consist of noble gasses, with helium and xenon receiving the most attention. They have a fast response and easily variable size and shape. The main disadvantage is their low light yield. The most common glass scintillators are cerium-activated silicate glasses containing lithium. They are widely used as neutron detectors. They are very robust, but sensitive to electrons and gamma rays and have quite low light yield.

4.3 Photomultiplier tube

Because the typical light output of a scintillation pulse is no more than a few hundred photons, a device capable of converting it to a usable corresponding electrical signal is required. Photomultiplier (PM) tube accomplishes this task very well without adding a large amount of random noise to the signal.

The simplified structure of a PM tube is illustrated in Fig. 4.2. The tube itself is usually made out of glass, because a vacuum inside is needed for efficient electron acceleration. There are two main components housed inside - a photocathode coupled to an electron multiplier structure. Their individual design and function will be now discussed. Typical types of PM tubes can be seen in Figure 4.3.

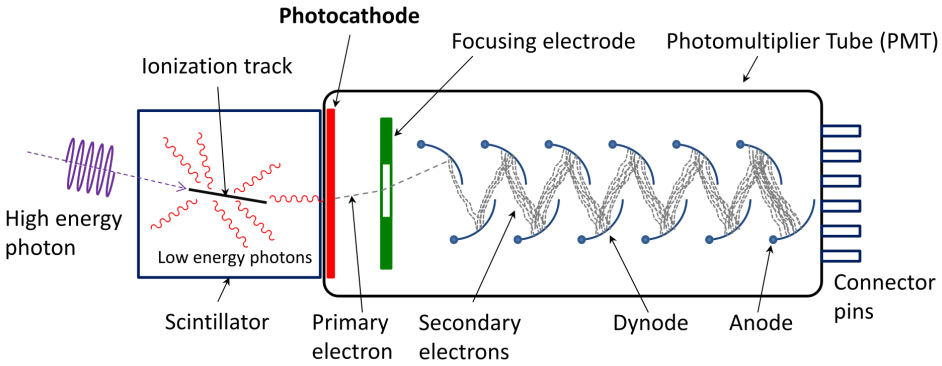

Figure 4.2: Schematic of a photomultiplier tube coupled to a scintillator.
By Qwerty123uiop, CC BY-SA 3.0, https://commons.wikimedia.org/w/index.php?curid=62426194

Figure 4.3: Typical types of PM tubes with different shape, structure, effective area, etc. Hamamatsu Photonics Deutschland GmbH, https://www.hamamatsu.com

4.3.1 The photocathode

The photocathode is a photosensitive layer that serves to convert the incident light photons to low-energy electrons. The produced photoelectrons will be of the same characteristic and have a similar time duration as the light signal coming from the scintillator. This conversion process can be described in three sequential stages.

In the first stage, the incident photon is absorbed and its energy is transferred to an electron within the photoemissive material. It is given by the quantum energy of the photon hv. In the second stage, electrons migrate to the surface, losing some of the energy through electron-electron collisions. Lastly, the electrons need to escape from the photocathode. They need to have enough leftover energy to overcome the inherent potential barrier that exists between any material and vacuum. It is often called *work function* and its value is more than 3 or 4 eV for most metals, but can be reduced to 1.5-2 eV using semiconductors.

4.3.2 The electron multiplier

The few photoelectrons produced by the photocathode are not sufficient for a convenient electrical signal. The electron multiplier serves as a near-ideal multiplier to increase their number. A typical pulse will give rise to 10^7-10^{10} electrons, which is enough to make the charge signal for the original scintillation event.

The electron multiplication is based on a process of secondary electron emission. Electrons are accelerated in a potential field and caused to strike the surface of an electrode, called the *dynode*. The kinetic energy of arriving electrons is determined almost entirely by the positive potential held on the dynode (typically several hundred volts). If the right conditions are met, the energy deposited by each electron can result in the reemission of several new electrons. Still, most of the new electrons do not contribute to the final secondary electron yield. The direction of motion of these excited electrons is essentially random and many of them will not reach the surface. Furthermore, some of them will not have enough energy to overcome the potential barrier at the surface.

For a single dynode, there is an overall multiplication factor δ given by the number of secondary electrons emitted per primary incident electron. For an optimum incident energy near 1 keV for conventional dynode materials (BeO, MgO, Cs_3Sb), the maximum multiplication factor is about 10. For the conventional dynode voltage of a few hundred volts, the value is typically 4-6. Clearly, one dynode will not be enough to achieve electron gains in the order of 10^7. Therefore, all PM tubes have multiple stages of them (see Fig. 4.2). Each dynode attracts electrons leaving the stage before and produces δ secondary electrons for each of the incident one. Since the newly created electrons have very low energies, they are quite easily guided to the next dynode. The overall gain for N stages is then simply given by

$$OG \approx \alpha\delta^N \tag{4.2}$$

where α is the number of photoelectrons collected by the multiplier structure. Hence, for a typical $\delta = 5$, ten stages will result in an overall gain of 5^{10}, or about 10^7. More advanced high-yield dynodes with $\delta = 55$ exists, that are capable of the same gain with only four stages.

In order for PM tubes to work properly, the photocathode and each succeeding multiplier stage must be connected to an external voltage, such that they are correctly biased with respect to each another. A positive voltage on the first dynode with respect to the photocathode is required to attract electrons between them. Similarly, each succeeding dynode must be held at a positive voltage with respect to the preceding one. Additionally, the voltage between the photocathode and the first dynode is often several times greater as between the next dynode stages. These voltage differences are usually provided by a resistive voltage divider and a single source of high voltage, as illustrated in Fig. 4.4.

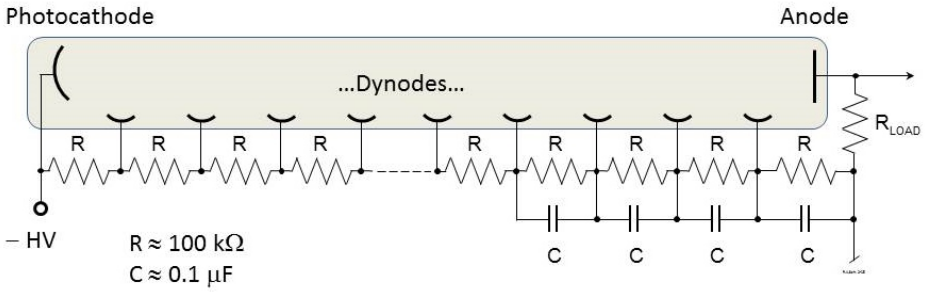

Figure 4.4: Typical PM voltage divider circuit using negative high voltage.
By Qwerty123uiop - Own work, CC BY-SA 4.0,
https://commons.wikimedia.org/w/index.php?curid=38349029

Because the electrons traveling from stage to stage have a low average energy (on the order of 100 eV), they are particularly sensitive even to the earth's magnetic field. Any manipulation near equipment with stray magnetic fields will have an appreciable effect on their trajectories. This problem is commonly solved with a magnetic shield in the form of a cylinder of mu-metal around the glass envelope of the PM tube.

Chapter 5

Experimental testing of PM tubes

Even though a pair of seemingly identical PM tubes should behave the same, in reality, it is not usually true. Two same PM tubes can be placed side by side and deliver different results. Knowing how individual PM tubes behave under certain circumstances can be very useful and can mean the difference between obtaining meaningful data from an experiment versus not having anything.

To evaluate the dynamic range of PM tubes, their sensitivity, and other attributes, two independent experiments were conducted. Firstly, PM tubes were tested on the PFZ-200 device, detecting pulses of hard X-rays (HXR) and neutrons. Secondly, PM tubes' gain and transition time were evaluated using a neodymium laser. Overview and results of both experiments will be now discussed.

5.1 PFZ-200 experiment

In the laboratory of high current discharges at the Department of Physics of FEE CTU in Prague, scintillation detectors with PM tubes are one of the major diagnostics to obtain data from experiments on the plasma focus PFZ-200. Due to the unpredictable nature of such experiments, having a wide range of correctly setup detectors is vital.

Each shot of the PFZ-200 device produces a pulse of HXR followed by a neutron pulse. Figure 5.1 shows such an example, where the first peak of HXR serves as a time marker and the second peak is the neutron signal. When the PM tube sensitivity is not set correctly, the lead shielding of the detector is not sufficient or the HRX pulse is very strong, the last dynode in the PM tube can get saturated. If this occurs, the PM tube may not be "ready" to process the succeeding neutron signal due to its relaxation time. In this case, the neutron pulse can be captured incompletely and be practically useless (see Fig. 5.2). Because plasma foci (as PFZ-200) are used to study fusion in plasma where neutrons carry important information about the event, not having information about them can jeopardize the experiment. However, this can be prevented by correctly setting PM tube supply voltage. Additionally, knowing the average amplitude of the signal at a certain voltage setting can be used to correctly set up the oscilloscope, so that the whole signal can be captured.

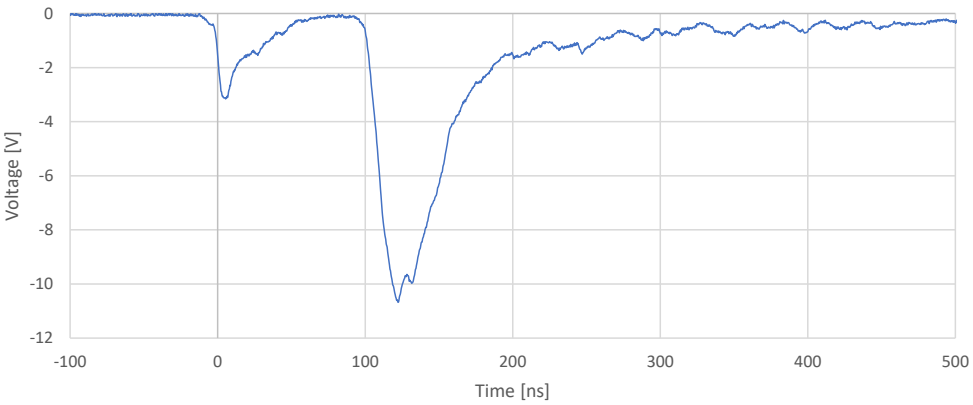

Figure 5.1: Exemplary signal from scintillation detector on the PFZ-200. The first peak around 0 ns are the HXR and the second dual peak are the neutrons from two consequent pinches.

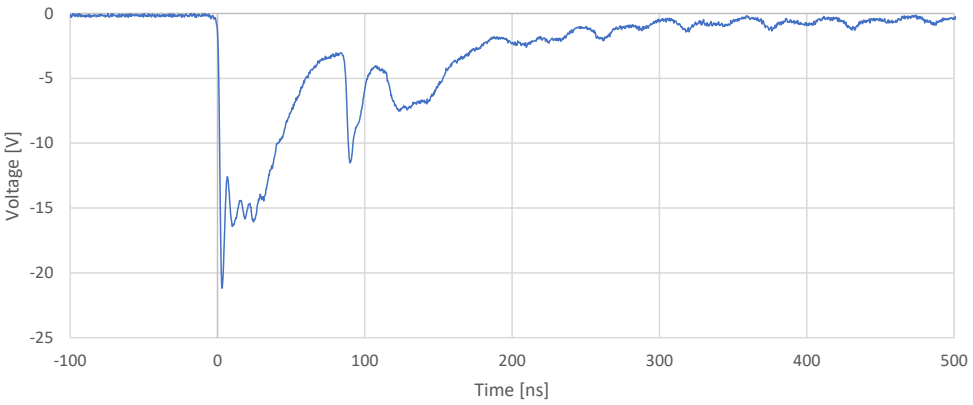

Figure 5.2: Exemplary signal from scintillation detector on the PFZ-200 where the PM tube got saturated.

5.1.1 Experiment setup

In total, four PM tubes HAMAMATSU R1828-01 (assembly H1949-51) were used. They were coupled together with a scintillator BC-408 from Saint-Gobain Crystals to make a scintillation detector (see Fig. 5.3). To partially suppress the incoming HXRs, each detector was put in a lead tube with a 4 mm thick wall. In a later stage of the experiment, an additional 2 mm lead sheet was put in front of the detectors. All four devices were put side by side in the EMP safety cabin (see Fig. 5.4), pointing towards the PFZ-200 device 269 cm in front. Upon triggering the PFZ-200 shot, outputs from the detectors were recorded using the Tektronix 5 series oscilloscope (1 GHz, 6.25 GS/s). To count the number of neutrons produced in each shot, a silver activation counter (Fig. 3.2) was used, placed 40 cm from the PFZ-200.

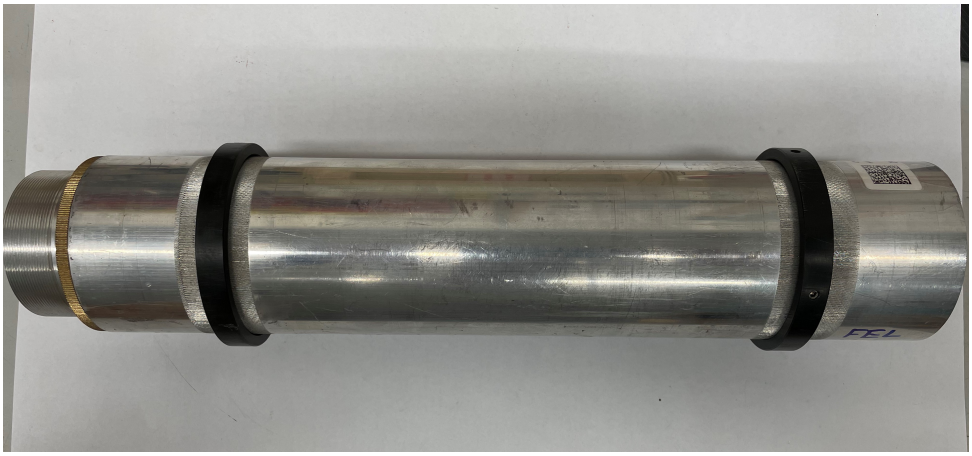

Figure 5.3: Scintillation detector in its housing.

Figure 5.4: Setup of four scintillation detectors in a Faraday cage, numbered PM1-PM4 from the left.

5.1.2 Results

All PM tubes were tested for two values of supply voltage, 1.4 kV and 1.2 kV. Eleven shots on the PFZ-200 device for each voltage value were performed. Since the amplitudes of the HXRs were in general greater than for the neutrons, a comparison of them for each individual detector is in place. Additionally, the PM tubes got several times saturated, which has a corresponding value. Because the silver activation counter can give the absolute neutron count reference, the linearity of neutron signals of the PM tubes can be tested as well.

Sensitivity and saturation

The first comparison at 1.4 kV PM tube supply voltage can be seen in Figure 5.5. After shot number 4, an additional 2 mm lead sheet was added in front of the detectors. However, it did not fully cover the rightmost detector (tube PM4), which was corrected by another 2 mm lead shielding after shot number 9. The difference of the shielding can be clearly seen in the results. In shots 1 and 4, all PM tubes got saturated (indicated by the red arrows). The saturation of PM4 in shot seven can be explained by the insufficient shielding. The last two shots showed an exceptional HXR intensity, therefore getting saturated.

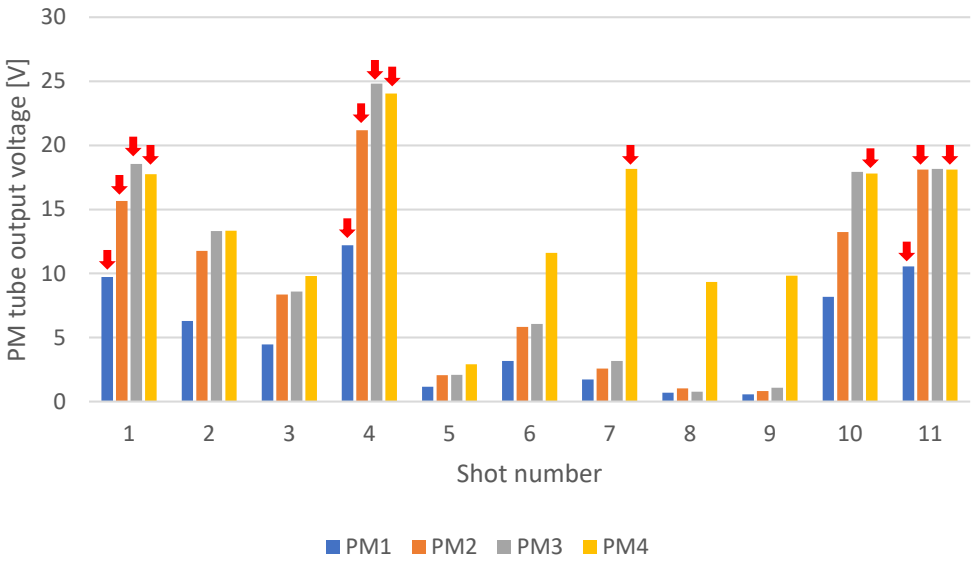

Figure 5.5: HXR signal amplitude comparison of four used PM tubes at 1.4 kV supply voltage. The red arrows marks a signal where the PM tube was in saturation.

The second comparison at 1.2 kV PM tube supply voltage can be seen in Figure 5.6. The 2 mm lead sheet was added after shot number 4, but the insufficient coverage of tube PM4 was not addressed in this case. Three shots were discarded due to the very low amplitude of HXR signal. As can be seen, the first 3 shots got all PM tubes into saturation. However, in those cases the HXR pulse was exceptionally long, with the FWHM (full width at half maximum) almost 40 ns instead of the typical 10-20. This explains why the PM4 in shot 5 was not saturated (indicated by a star), because the FWHM was in the typical range.

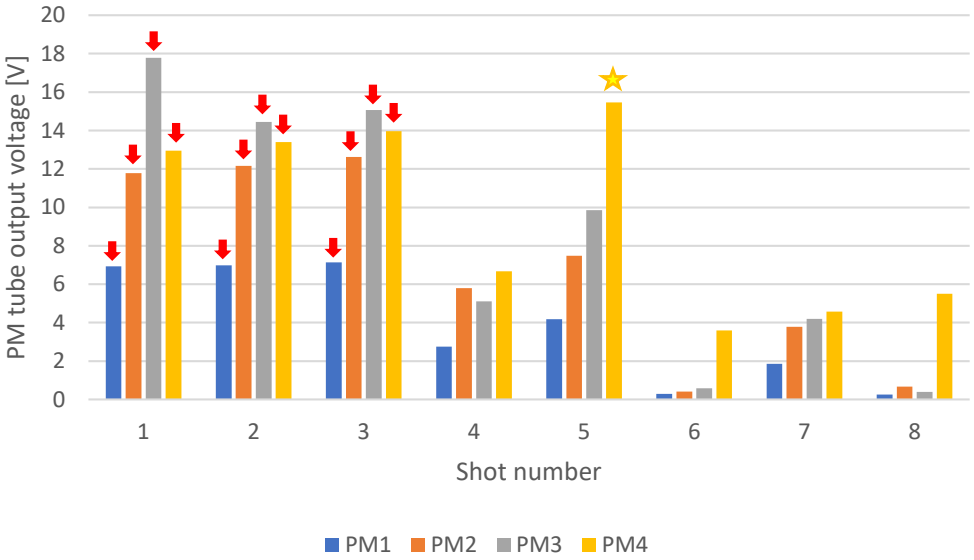

Figure 5.6: HXR signal amplitude comparison of four used PM tubes at 1.2 kV supply voltage. The red arrows marks a signal where the PM tube was in saturation.

From these findings, it can be concluded that even though all PM tubes should be the same, there is a difference between them. Mind that the distance between them and the PFZ-200 was the same, so they should have received the same amount of incident radiation. The PM3 seems to be the most sensitive one, but overall PM2, PM3, and PM4 behaved very similarly regardless of the supply voltage. The PM4 differences are due to the uneven shielding mentioned above. The greatest difference is in the performance of tube PM1, which is clearly the least sensitive one.

Because there is a high variation between the saturated and unsaturated signals, it can not be precisely concluded at what output voltages are the PM tubes in saturation. Only for the PM3 it can be assumed (shots 1, 10, 11 in Fig. 5.5), that the PM tube gets into saturation between the output voltages of 18.17 - 18.55 V in the case of PM tube supply voltage at 1.4 kV. The difference in the signals of the other PM tubes and supply voltage is making any assumptions inconsequential.

Linearity

For each shot of the PFZ-200, a neutron count from the silver activation counter was recorded. The total neutron yield can be then calculated using this formula

$$Y = 4\pi r^2 k(C - B) \tag{5.1}$$

where $r = 40$ cm is the distance from the plasma focus, $k = 4.69$ is a calibration constant, C is the counter output, and $B = 60$ is the natural radiation background. Since neutron production from the plasma focus is generally assumed to be cylindrically symmetric, the same amount of neutrons reaching each detector can be expected. For each neutron signal of the PM tube, the area under the curve can be calculated from the measured data. It is proportional to the neutron yield obtained by the moderator counter. Therefore, the plot of the area and the neutron yield values should be overall linear, unless the PM tube gets saturated. The graph would then flatten on top.

To calculate the area under the neutron signal, a semiautomatic algorithm was created using MATLAB environment. Because of the inconsistent nature of the pulses, the time of the beginning of the signal had to be added manually. The total integration time of 100 ns was chosen, as it reliably includes the main neutron signal. Some shots had to be discarded, because the saturation of PM tube by HXRs corrupted the following neutron signal (see Fig. 5.2).

The results for PM tube supply voltage 1.4 kV and 1.2 kV can be seen in Figures 5.7 and 5.8, respectively. As can be seen, the individual results are very scattered. The fluctuations are due to the small sample size and mainly because the scintillation detectors have quite large uncertainty in absolute value count compared to the silver activation counters. Hence the reason they are preferably used.

Better visualization of the results can be made using least squares linear regression. The slope of the line corresponds to the calibration constant, which can be used to calculate the absolute neutron count, like in case of the silver activation counter. If the results are compared with the findings from the section above, similar conclusions about the PM tubes can be made. Tubes PM2, PM3, and PM4 behaved again a lot alike. In this case, PM2 seems to be the most neutron sensitive and PM1 is clearly underperforming from the rest.

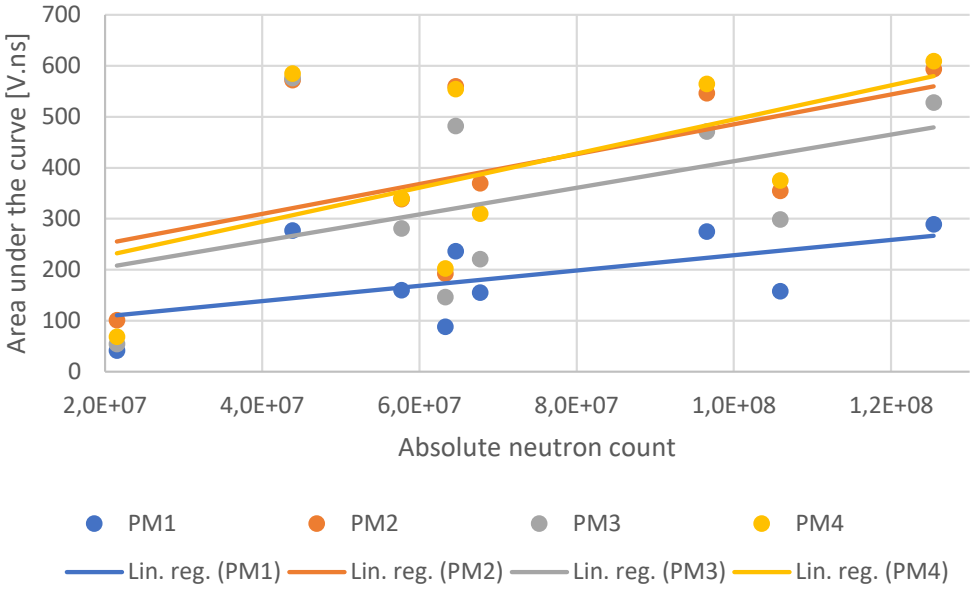

Figure 5.7: Dependence of the neutron signal from the PM tubes on the total neutron yield at 1.4 kV PM tube supply voltage.

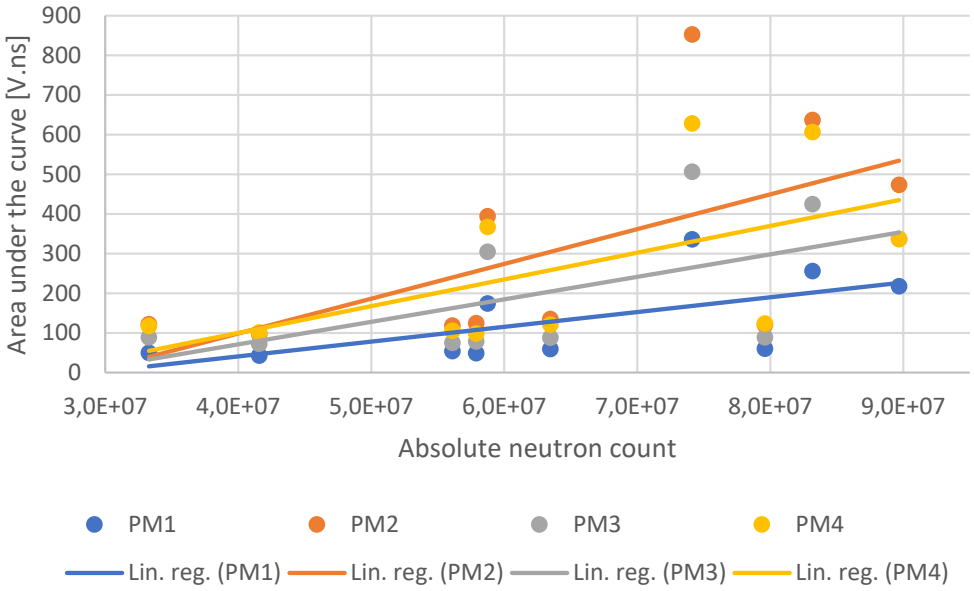

Figure 5.8: Dependence of the neutron signal from the PM tubes on the total neutron yield at 1.2 kV PM tube supply voltage.

5.2 Neodymium laser experiment

Since plasma focus experiments are in general very unpredictable, the use of a laser as a source of an input signal allows a more methodical approach. However, knowing the exact properties of light requires quite sophisticated

measurements. Fortunately, for the purposes of this experiment, only the fact of consistent input signal is sufficient. The PM tube response can be compared to an output signal of, for example, a photodiode to determine its relative gain. Even though the measurement is relative, it is very useful in practice, if the PM tube sensitivity needs to be changed during the experiment. Having another signal reference can be also used to measure the transition time of the PM tube, which is the time needed for the signal amplification. Knowledge of the transition time is important for precise synchronization of the PM tube.

5.2.1 Experiment setup

The experiment was setup according to the scheme in Figure 5.9. The neodymium laser was set to pulse mode, lowest power, and wavelength of 532 nm. The beam was directed through a filter to further reduce its power to match the PM tube capabilities. Additionally, its width was expanded 10 times from 2 mm to 20 mm, so it could be more easily captured. The beam then reached the entry of the optical cable leading to the PM tube and the photodiode. Both signals led to the Tektronix series 5 oscilloscope, again through optical cables. This time, a total of five PM tubes HAMAMATSU R1828-01 (assembly H1949-51) were tested. Except for the surplus one, the labels are matching the previous results. The PM tubes were powered by a adjustable voltage source.

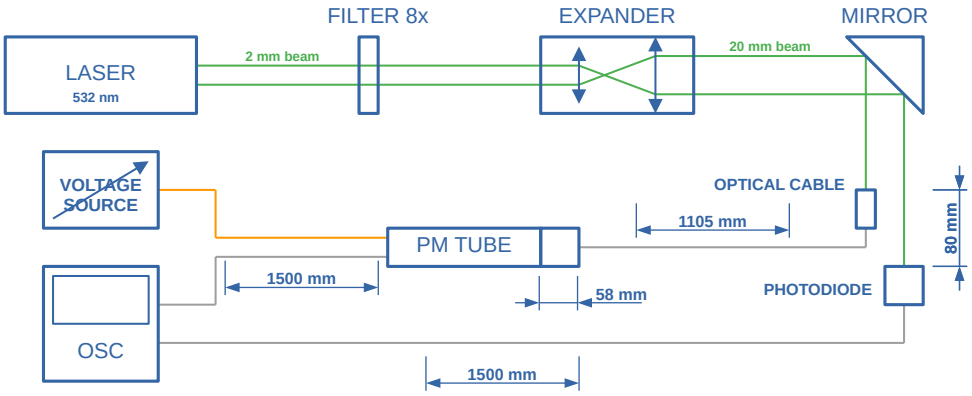

Figure 5.9: Block scheme of the experiment setup with cable measurements.

5.2.2 Results

The five PM tubes were tested with 27 different voltage settings, ranging from 700 V to 2000 V. The laser was fired 2 times for each voltage level. The resulting typical signals can be seen in Figures 5.10 and 5.11.

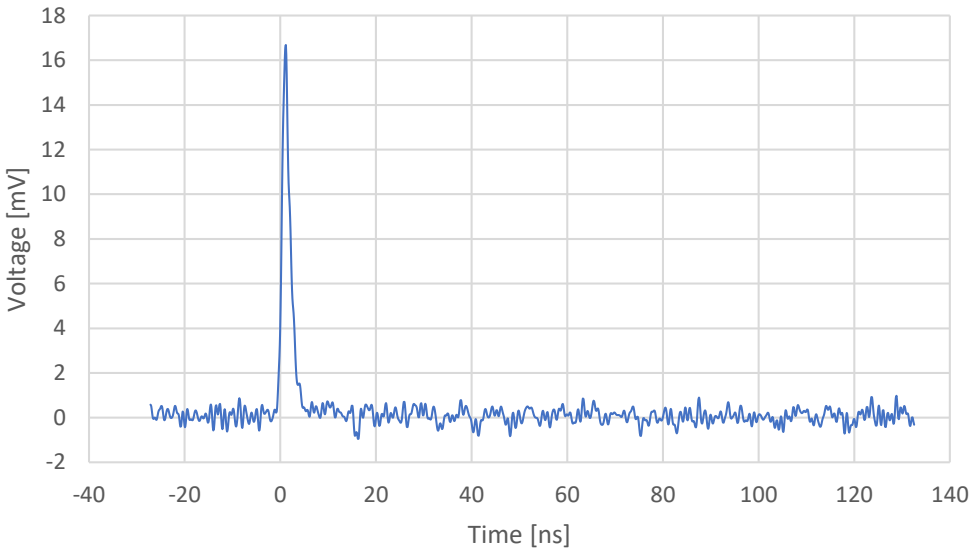

Figure 5.10: Response of the photodiode to the laser pulse.

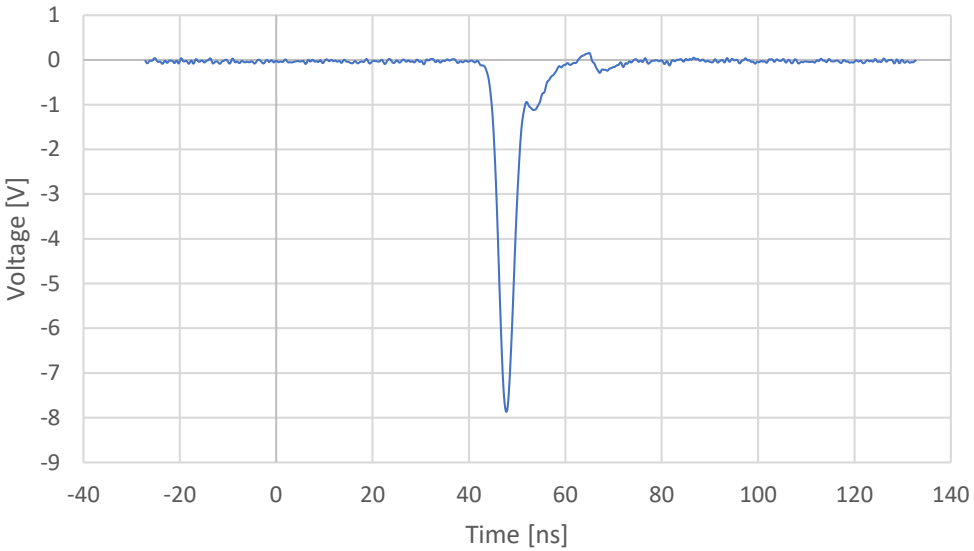

Figure 5.11: Response of the PM tube to the laser pulse.

Relative gain

This time, the nature of the data allowed for an automatic processing algorithm to be implemented, again using MATLAB environment. The algorithm finds extremes for both the PM tube and the photodiode signal (maximum and minimum respectively) and computes the relative gain as follows

$$A = \frac{U_{PM\ tube}}{U_{photodiode}} \tag{5.2}$$

Since it is relative, the units are set arbitrarily. Then it processes the results so they are put in an excel sheet, where they can be worked on. Figure 5.12 compares the relative gain between each PM tube. To better visualize the gain per individual supply voltage, a logarithmic scale was applied to the Figure 5.13. There is a gap in values of the PM4 tube, because the data in this section were corrupted.

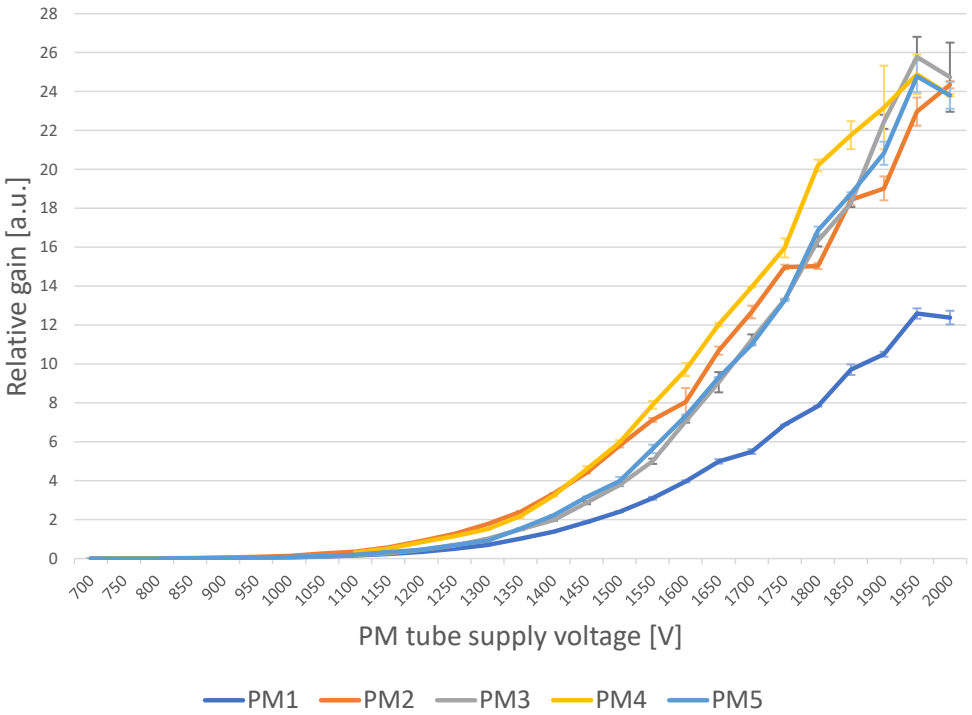

Figure 5.12: Effect of supply voltage on the relative gain of the PM tubes.

There is a similar trend in the result as in the PFZ-200 experiment. Again, the PM1 tube is the most different one, having the lowest overall relative gain. The rest behaves very alike, where PM3 and PM5 are almost identical and with consistent gain across.

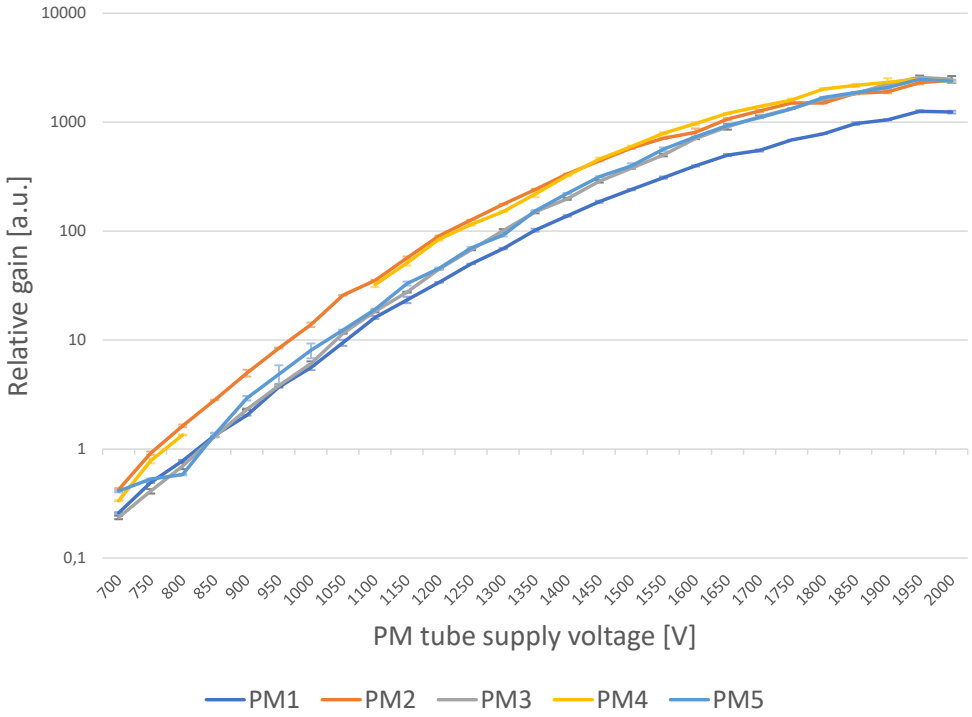

Figure 5.13: Comparison of the gain results in logarithmic scale.

Transition time

Similarly to the section above, the automatic algorithm was used to process the data. To calculate the transition time, the time it takes for the photons to reach the oscilloscope through the cables connecting the PM tube and the photodiode to the oscilloscope is required. This can be determined from the cable lengths (see Fig. 5.9) and the speed of light through them. The last information needed is the interval between the arrival of each signal in the oscilloscope. When added to the PM tube cable time, the photodiode cable time can be subtracted from the result. The difference corresponds to the unknown section of the path the signal has taken, the PM tube transition time. The equation is

$$t_{transition} = (t_{PMT} + t_{PMT-PD}) - t_{PD} \tag{5.3}$$

where t_{PMT} and t_{PD} are times the signal traveled through the PM tube and the photodiode cable path, respectively. t_{PMT-PD} is the time between the signals in the oscilloscope. The algorithm finds the peaks of both signals and the time they arrived, computes the difference, and finds the transition time. The results for all PM tubes at different voltage levels are in Figure 5.14.

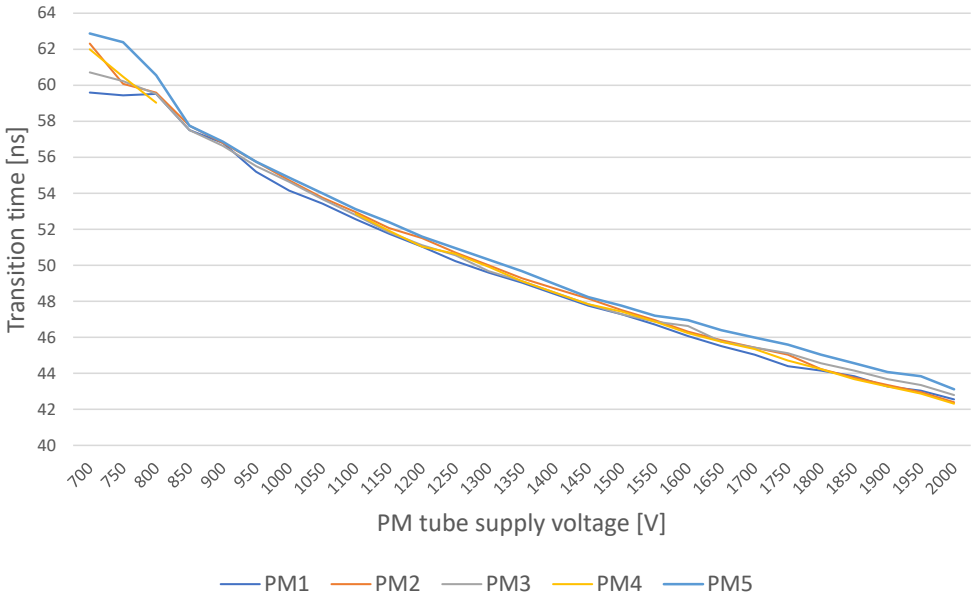

Figure 5.14: Effect of supply voltage on the transition time of the PM tubes.

As expected, the higher the supply voltage, the shorter the transition time is, because the greater potential between the dynode stages makes the electrons move faster. All PM tubes had very similar results. Since the transition time depends mainly on the electron speed and the distance traveled, it can be concluded that their voltage dividers work almost identically and the construction of the PM tubes in terms of their dimensions is also very uniform.

5.3 Discussion

The results of both experiments clearly show that all PM tubes, even though of the same type, behave differently to some extent. Knowledge of those differences is important to correctly set and synchronize these devices.

The experiments on the PFZ-200 show that the dynamic ranges of all four tested PM tubes differ. From their response to the incoming HXRs at different supply voltages it is clear that tube PM1 has the lowest sensitivity, significantly deviating from the rest. This is further back up by the evaluation of neutron signals and the measuring of the relative gain using neodyminum laser. Overall, tubes PM2 to PM5 are approximately 2 times as sensitive as the PM1. The distinction is more evident with the increasing supply voltage.

Due to the insufficient sample size, the exact level of saturation of individual PM tubes cannot be pointed out. However, the results at 1.2 kV supply voltage show that with the amount of lead shielding used and typical FWHM, the signals from PFZ-200 are fully captured within the acceptable range and with no saturation.

Even though there is a higher uncertainty in measuring absolute neutron count using the scintillation detectors, the approximation of the data shows overall linearity. This is within the expectations and could be further improved by higher sample size.

Lastly, the transition time of the PM tubes was measured. As expected, the results are very similar, because the voltage divider should not change across the PM tubes. The transition time decreases with increasing supply voltage, which is consistent with the theory.

As mentioned above, there are clear differences between the measured PM tubes, mainly the PM1. The main cause of that is probably the degradation of the photocathode, which is the most aging sensitive component. This should be taken into consideration when using these diagnostic devices, as it can lead to inconclusive experiment results. This issue can be, however, solved by evaluating the dynamic range of the PM tubes and adjust the experiment setting accordingly.

Chapter 6

Conclusion

The study of neutron-involving phenomenons is a highly discussed topic, where precise diagnostic tools are required. Photomultiplier (PM) tubes play a crucial role here, because signals from such events are often very weak. To obtain any data for them, they need to be converted to an electrical signal, which would be, without any amplification, insufficient to work with.

The theoretical part of this thesis includes the processes of neutron production, methods of neutron detection, and the description of the scintillation detector which includes the PM tubes. The experimental part aims to evaluate the dynamic range, relative gain, and transition time of several PM tubes used for neutron detection in the Plasma Focus Laboratory at the Department of Physics FEE CTU and to point out the differences between them which was done successfully.

It was shown how the PM tubes behaved at different supply voltages and how they response to different types of incident radiation, namely, hard X-rays, neutrons, and light. For that purpose, two independent experiments were conducted using a plasma focus PFZ-200 device and a neodymium laser, testing the same type of four and five PM tubes, respectively. Data from the first experiment showed how different is the sensitivity and level of saturation of each PM tube in response to the same input signal. Using a silver activation counter, the linear dependence of the PM tube neutron signal on the total neutron yield was demonstrated. The second experiment evaluated the relative gain differences between the PM and their transition time.

The results of both experiments concluded that there were clear differences between the tested PM tubes, even though they are of the same type and were tested in the same conditions. There was particularly one PM tube that showed twice as low sensitivity than the rest. This conclusion was the same in both experiments. A larger data set in the first one would be required to determine more specific levels at which the saturation occurs. The reason for the inconsistencies between the PM tubes was narrowed down to the degradation of the photocathode. All results can be used to correctly set and synchronize the PM tubes in upcoming experiments and the data processing methods to further evaluate them further.

Continuing this work, a calibration of the whole detector, including the scintillator, could be done using a calibration source of radiation, for example, a cyclotron. The dynamic range of the PM tubes could be further increased by using a better voltage divider with higher capacity and logarithmic division instead of linear. This would further increase the level at which the PM tube is saturated. The used semiautomatic and automatic algorithms could be expanded further by a user-friendly interface, which could simplify the operation of the PFZ-200 device and automatically process the data straight from the oscilloscope.

Bibliography

[1] Marek Scholz. *Plasma-Focus and Controled Nuclear Fusion.* Institute of Nuclear Physics PAN, 2014.

[2] S. G. Pinto. GEM Application Outside Hight Energy Physics. *Modern Physics Letters A*, January 2013.

[3] Glenn. F. Knoll. *Radiation Detection and Measurement, Third Edition.* John Wiley and Sons, 2000.

[4] John B. Birks. *The theory and practice of scintillation counting.* Pergamon Press, Ltd., 1964.

[5] M. J. Sadowski. Important problems of future thermonuclear reactors*. *Nukleonika -Original Edition- 60(2)*, June 2015.

[6] Mikhail I. Pergament. *Methods of Experimental Physics.* CRC Press, 2015.

[7] Pavel Kubeš. *Impulsní silnoproudé výboje a jejich diagnostika.* 2004.

[8] Robert W. Conn. Nuclear fusion. *Britannica*, April 2016.

[9] J. Cikhardt et al. Neutron Spectrum Measured by Activation Diagnostics in Deuterium Gas-Puff Experiments on the 3 MA GIT-12 Z-Pinch. *IEEE Transactions on Plasma Science*, 45, December 2017.

[10] Jakub Cikhardt. High Energy Density Plasma Diagnostics Using Neutron and Gamma Detectors. *Department of Physics, FEE CTU*, November 2017.

[11] T. D. McLean H. ING, R. A. Noulty. Bubble Detectors - A Maturing Technology. *Pergamon*, November 1996.

[12] H. Thierens F. Vanhavere, M. Loos. The lifespan of the BD-PND bubble detector. *Radiation Protection Dosimetry*, 85, September 1999.

[13] D. Klír et al. Review of Scientific Instruments. *AIP Publishing*, 82:2, March 2011.

[14] K. Řezáč et al. Improvement of time-of-flight methods for reconstruction of neutron energy spectra from D(d,n)^{3}He fusion reactions. *IOP Publishing*, September 2012.

[15] William R. Leo. *Techniques for Nuclear and Particle Physics Experiments*. Springer, 1994.

[16] M. Nikl V. Jarý. Novinky ve světě scintilačních materiálů. *Fyzikální ústav AV ČR*, 63.

[17] H. I. West et al. Detection of X-Rays by Means of NaI(Tl) Scintillation Counters. *Physical Review*, 81, November 1950.

BACHELOR'S THESIS ASSIGNMENT

I. Personal and study details

Student's name: **Veškrna Daniel** Personal ID number: **483632**

Faculty / Institute: **Faculty of Electrical Engineering**

Department / Institute: **Department of Control Engineering**

Study program: **Cybernetics and Robotics**

II. Bachelor's thesis details

Bachelor's thesis title in English:

Dynamic range of photomultipliers in pulse mode

Bachelor's thesis title in Czech:

Dynamický rozsah fotonásobičů v impulsním režimu

Guidelines:

The bachelor thesis should include an appropriate introduction covering the neutron detection methods and the principle of neutron production at plasma focus devices.
- The practical part of the thesis aims to experimentally evaluate the dynamic range of photomultiplier tubes used for neutron detection in the Plasma Focus Laboratory at the Department of Physics FEE CTU.
- Differences in the dynamic range and sensitivity of individual photomultipliers (model R1828-01) have to be assessed.
- In these considerations, take into account dependence on the photomultiplier supply voltage.
- If the character of the signals including the noise makes it possible, try to process the experimental data using an automatic or semi-automatic method.

Bibliography / sources:

[1] Glenn F. Knoll: Radiation Detection and Measurement, 4th Edition, ISBN: 978-0-470-13148-0, USA 2010
[2] Mikhail I. Pergament: Methods of Experimental Physics, ISBN: 978-0367866426, Boca Raton 2019
[3] Daniel Klir, et al.: Fusion neutron detector for time-of-flight measurements in z-pinch and plasma focus experiments, Review of Scientific Instruments 82, 033505, 2011
[4] Jakub Cikhardt: High Energy Density Plasma Diagnostics Using Neutron and Gamma Detectors, Doctoral thesis, Prague 2017
[5[Pavel Kubeš: Impulsní silnoproudé výboje a jejich diagnostika, Praha 2004
[6] Marek Scholz: Plasma-focus and controlled nuclear fusion, ISBN 978-83-63542-24-5, Kraków 2014.

Name and workplace of bachelor's thesis supervisor:

Ing. Jakub Cikhardt, Ph.D., Department of Physics, FEE

Name and workplace of second bachelor's thesis supervisor or consultant:

Date of bachelor's thesis assignment: **26.01.2021** Deadline for bachelor thesis submission: **21.05.2021**

Assignment valid until:
by the end of summer semester 2021/2022

Ing. Jakub Cikhardt, Ph.D.	prof. Ing. Michael Šebek, DrSc.	prof. Mgr. Petr Páta, Ph.D.
Supervisor's signature	Head of department's signature	Dean's signature

III. Assignment receipt

The student acknowledges that the bachelor's thesis is an individual work. The student must produce his thesis without the assistance of others, with the exception of provided consultations. Within the bachelor's thesis, the author must state the names of consultants and include a list of references.

. _____
Date of assignment receipt

_____
Student's signature